Thermal Transitions of Montmorillonite/ Polyurethane Nanocomposites

Y. I. Tien and K. H. Wei*

Department of Materials Science and Engineering, National Chiao Tung University, Hsinchu 30049, Taiwan, R.O.C.

Received June 15, 2000; revised September 7, 2000; accepted November 16, 2000

Abstracts: The hard-segment phase thermal transitions and heat-resistance of benzidine-modified-montmorillonite (BZD-Mont)/polyurethane nanocomposites of different hard segment contents were found to be affected by a small amount of BZD-Mont. In particular, the presence of less than 5 wt% layered silicates from BZD-Mont can result in hard segments not only having a more thermally stable long-range order and a higher melting temperature, but also showing a loss of crystallinity of the hard segment in polyurethane. Additionally, the degradation temperature of BZD-Mont/polyurethane nanocomposite was slightly higher than that of pure polyurethane.

Keywords: Montmorillonite, Nanocomposites, Polyurethane, Thermal transitions.

Introduction

Thermoplastic polyurethane is a copolymer with - $[S\text{-}H]_m$-type chain architecture where S and H are the soft- and hard- segment sequences, respectively. Due to the difference in the chemical structure, the two kinds of segment sequences usually segregate and form an aggregated pseudo-two-phase morphology [1-4]. The soft segment is typically flexible at room temperature because of its low glass transition temperature, while the hard segment is either a glassy or a crystalline material. The glass transition temperature of the soft phase and the multi-endothermic behavior of the hard phase of polyurethane have been investigated previously [5,6]. The endothermic peak in the range of 140 to 200 °C for polyurethane has been associated with the destruction of the long-range order of an unspecified nature, while the endotherm observed above 200 °C is generally attributed to the melting of the microcrystalline regions of the hard-segment phase of polyurethane. After the hard-segment phase melts, polyurethane gradually starts to degrade from the urethane bond of the hard segments through various mechanisms [7-9].

Montmorillonite is an inorganic material consisting of negatively-charged layered silicates which form ionic bonds with cations in the intergalleries of the silicates. Hence, montmorillonite shows no affinity for hydrophobic organic polymers. Organic molecules, usually termed swelling agents, containing cation functional groups were used to render the normally hydrophilic silicate surface organophilic through ion exchange with the cations between the layered silicates. Several montmorillonite/condensation polymer nanocomposites have been synthesized successfully, including montmorillonite/Nylon 6 [10-13], montmorillonite/polyimide [14-17], montmorillonite/polycaprolactone [18-19], and montmorillonite/polyethylene terephthalate [20]. Recently, montmorillonite/polyurethane nanocomposites [21-24] have been developed in several laboratories, including our own, and their degree of phase separations were characterized by Fourier transform infrared spectroscopy [25]. As an extension of previous studies, the thermal properties of montmorillonite/polyurethane nanocomposites at different hard segment ratios were investigated in this study.

Experimental Section

1. Materials

Wyoming Na^+-montmorillonite, Source clay Swy-2, was obtained from the Clay Minerals Depository at the University of Missouri, Columbia, MO, USA. Swy-2 Na^+-montmorillonite having a

*To whom all correspondence should be addressed.
Tel: 886-3-5731871, Fax: 886-3-5724727
E-mail: khwei@cc.nctu.edu.tw

J. Polym. Res. is covered in ISI (CD, D, MS, Q, RC, S), CA, EI, and Polymer Contents.

Table I. Compositions of polyurethanes and BZD-Mont/polyurethane nanocomposites.

	MDI/1,4-BD/PTMEG (molar ratio)	BZD-Mont ratio (wt%)
PU39	2/1/1	0
1/99 BZD-Mont/PU39	2/1/1	1
3/97 BZD-Mont/PU39	2/1/1	3
5/95 BZD-Mont/PU39	2/1/1	5
PU50	3/2/1	0
1/99 BZD-Mont/PU50	3/2/1	1
3/97 BZD-Mont/PU50	3/2/1	3
5/95 BZD-Mont/PU50	3/2/1	5
PU63	5/4/1	0
1/99 BZD-Mont/PU63	5/4/1	1
3/97 BZD-Mont/PU63	5/4/1	3
5/95 BZD-Mont/PU63	5/4/1	5

cationic exchange capacity 76.4 meq/100 g was screened with a sieve of 325-mesh to remove impurities. 10 g of the screened montmorillonite was gradually added to a previously prepared solution of 0.89 g benzidine dissolved in 1000 mL of 0.01 N HCl at 60 °C, and the resultant suspension was stirred vigorously for 3 hrs. The treated montmorillonite was repeatedly washed by de-ionized water. The filtrate was titrated with 0.1 N $AgNO_3$ until there was no further formation of AgCl precipitate and in order to ensure a complete removal of chloride ions. The filtered cake was then placed in a vacuum oven at 80 °C for 12 hrs drying. The dried cake was ground and screened with a 325-mesh sieve to obtain the benzidine-modified-montmorillonite that was termed BZD-Mont.

Polytetramethylene glycol (PTMEG, M_n = 1,000, Aldrich) was dehydrated in a vacuum oven 60 °C for 2 days. 4,4'-Diphenylmethane diisocyanate (MDI, Aldrich) was melted and pressure filtered under N_2 at 60 °C followed by recrystallization from hexane in an ice bath. Dimethylforamide (DMF, 99%, Fisher) and 1,4-butane diol (1,4-BD, Lancaster) were dried over calcium hydride for 2 days and then were vacuum-distilled. Pure polyurethanes at different hard segment ratios were synthesized by a random one-step method in which MDI, 1,4-BD and PTMEG were directly mixed in DMF [1], and then the whole solution was heated to and kept at 90 °C for 3 hrs. The detailed steps of the synthesis have been described elsewhere [25].

2. Characterization

Wide angle X-ray diffraction (WAXD) experiments were performed using a Mac Science M18 X-ray diffractometer, and the diffraction curves were obtained from 3° to 40° at a scan rate of 1°/min. The samples for the transmission electron microscopy (TEM) study were first microtomed with a Leica Ultracut Uct into about 90 nanometer thick slices at -80 °C and then observed by TEM of JEOL-200FX. Thermal analyses of the samples were conducted with a Perkin-Elmer DSC-7 differential scanning calorimeter (DSC). The samples were heated from -100 to 240 °C at a heating rate of 20 °C/min under a helium purge. Thermogravimetric analyses (TGA) was conducted by heating the samples from 25 to 800 °C at a heating rate of 20 °C/min under an N_2 atmosphere by TGA 2950.

Results and Discussion

The compositions of pristine polyurethanes and synthesized montmorillonite/polyurethane nanocomposites are given in Table I. The wide-angle X-ray diffraction (WAXD) curves of the montmorillonite and the benzidine-modified-montmorillonite (BZD-Mont) are presented in Figure 1(a). In Figure 1(a), the *d*-spacings of the pristine montmorillonite and the BZD-Mont were 1.2 and 1.54 nm, respectively, indicating that the silicate layer galleries in the montmorillonite were intercalated by benzidine molecules. After mixing BZD-Mont with polyurethane in DMF, intercalated BZD-Mont/polyurethane nanocomposites were synthesized judging from both the WAXD patterns and transmission electron microscopy photographs as shown in Figure 1 (b) and 1(c), respectively. In Figure 1(b), there was no WAXD peak present between 2θ = 3~10° for 3/97 BZD-Mont/polyurethane nanocomposites at different hard segment ratios, verifying that the *d*-spacing was larger than 3 nm. The broad peaks at 2θ = 20° were due to the amorphous phase in polyurethane. In Figure 1(c), the space between the silicate layers (dark lines) was between 4~5 nm, indicating an intercalated structure. The variations in the molecular weights of recovered polyurethanes from these nanocomposites in our previous study [25] were less than 10%, implying that the length of the polyurethane molecular chain was not affected by the presence of the silicate layers. The DSC curves of montmorillonite/polyurethane nanocompoistes of different hard segment contents are shown in Figures 2 (a), 2(b) and 2(c), and the resultant soft-phase glass transition temperature (T_g), the long-range-order disruption temperature (T_L), the hard-phase melting temperature (T_m), the enthalpy change for long-range-order disruption (ΔH_L) and the enthalpy change during melting (ΔH_m) of pure polyurethane and montmorillonite/polyurethane nanocomposites are given in Table II. In Table II, for PU39 and PU50, the soft-phase glass transition temperature increased slightly with the hard segment content in polyure-

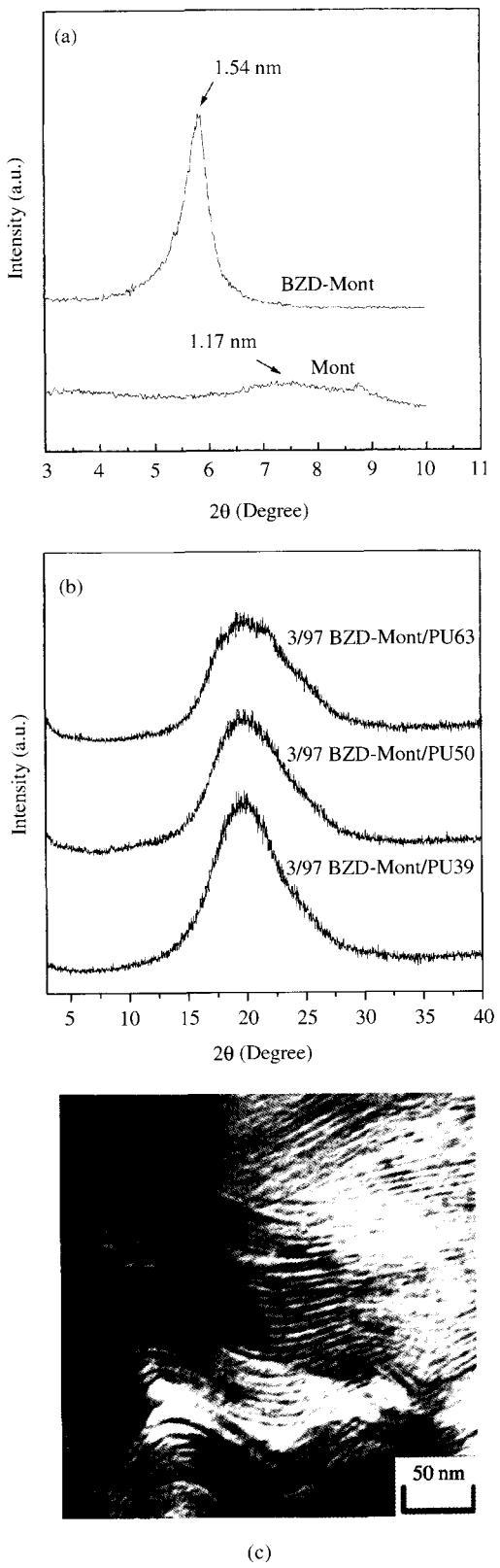

Figure 1. The wide-angle-X-ray-diffraction patterns for (a) benzidine modified montmorillonite (BZD-Mont) and montmorillonite (Mont), (b) 3/97 BZD-Mont/PU39, 3/97 BZD-Mont/PU50 and 3/97 BZD-Mont/PU63, and (c) transmission electron microscopy photograph of the cross section view of 1/99 BZD-Mont/PU50.

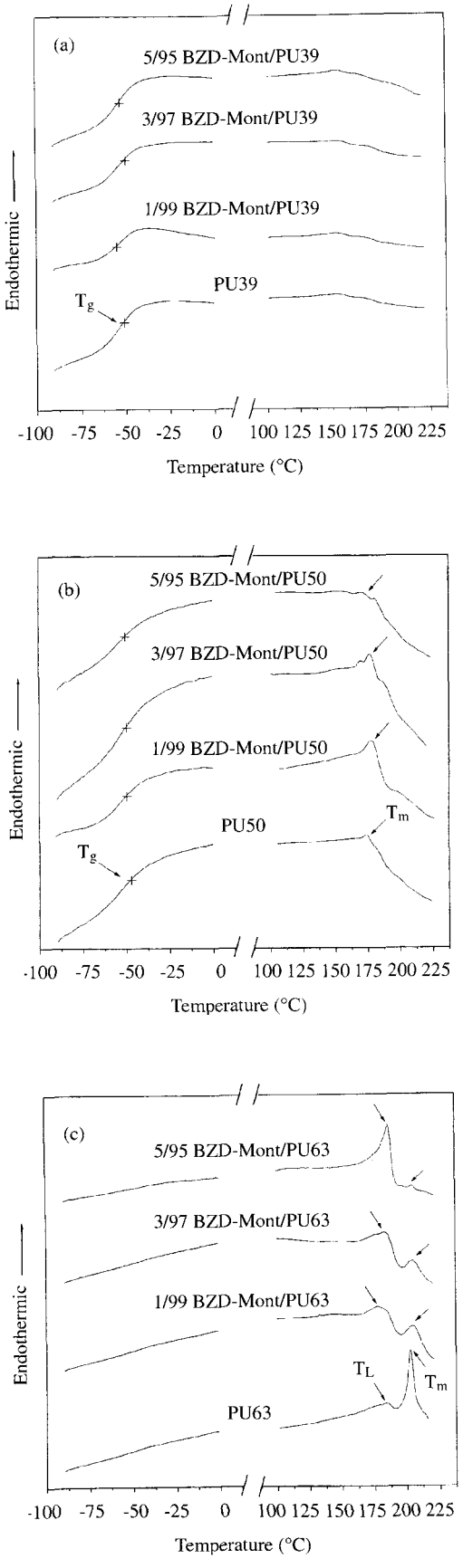

Figure 2. The DSC curves of pristine polyurethane and of BZD-Mont/polyurethane for (a) PU39, (b) PU50, and (c) PU63 cases.

Table II. Thermal properties of polyurethanes and BZD-Mont/polyurethane nanocomposites.

	T_g (°C)	T_L (°C)	T_m (°C)	ΔH_L (J/g)	ΔH_m (J/g)	T_d[(a)] (°C)
PU39	-53.0	*	*	*	*	320
1/99 BZD-Mont/PU39	-53.0	*	*	*	*	332
3/97 BZD-Mont/PU39	-51.6	*	*	*	*	342
5/95 BZD-Mont/PU39	-52.9	*	*	*	*	354
PU50-50.6	*	174.1	*	8.4	311	
1/99 BZD-Mont/PU50	-50.4	*	178.1	*	8.3	319
3/97 BZD-Mont/PU50	-49.1	*	176.5	*	6.9	326
5/95 BZD-Mont/PU50	-49.0	*	175.5	*	6.9	330
PU63 *	178.3	202.0	5.6	14.6	302	
1/99 BZD-Mont/PU63	*	180.3	206.0	13.4	5.0	310
3/97 BZD-Mont/PU63	*	184.0	204.4	16.1	4.3	315
5/95 BZD-Mont/PU63	*	186.5	203.5	23.4	1.0	317

*: Not detectable in the curves.
(a) Temperature at 5 wt% loss.

thane owing to the increasing degree of phase mixing [5]. The soft-phase of PU63 was not detectable in the DSC measurement. The variations in T_g of PU39 and PU50 nanocomposites were quite small, and it is possible that these small variations were caused by the fact that most BZD-Mont being distributed in the hard-segment phase because the residue isocyanate (–NCO) group in polyurethane could have reacted with the available amine ($-NH_2$) groups in the benzidine-modified-montmorillonite to produce urea.

There was no melting peak present for PU39, while the melting temperature of PU50 was 174.1 °C. This result was consistent with the previous result, where the crystallization of polyurethane occurred when the hard segment content was more than 45% [3]. For PU63, the long-range-order disruption temperature was 178.3 °C, and the melting temperature of the microcrystalline hard segment domain was 202.0 °C, corresponding to the fact that multiple endotherms appeared for polyurethane having more than 55% hard segment content [5].

The melting temperatures of PU50 nanocomposites increased to 178.1 °C at 1 wt% BZD-Mont content, but decreased to 176.5 °C at 3 wt% and to 175.5 °C at 5 wt% BZD-Mont content as compared to the melting temperature (174.1 °C) of pure PU50. The melting of the crystalline domain was buffered by the nearby silicates, and the molecular motion of polyurethane was restricted, causing an increase in its melting temperature. The maximum melting temperature occurred in PU50 nanocomposites containing 1 wt% BZD-Mont and can be attributed to a better dispersion of silicate in polyurethane at this particular silicates content, resulting in a maximum restriction effect on the melting of polyurethane. In the case of BZD-Mont/PU63, the long-range-order disruption temperature (T_L) increased with the amount of BZD-Mont, from 178.3 °C for pure PU63 to 186.5 °C for 5/95 BZD-Mont/PU63 as given in Table II. This phenomenon can be explained by the fact that the disruption of long-range order of the hard segment in PU63 was hindered by the presence of BZD-Mont during heating. The dependence of the hard-phase melting temperature of BZD-Mont/PU63 on BZD-Mont was similar to that of BZD-Mont/PU50.

The melting enthalpy changes (ΔH_m) of the hard segment phase were 8.4 and 14.6 J/g for PU50 and PU63, respectively, corresponding to the fact that the higher hard segment content resulted in higher crystallinity in polyurethane [4]. The melting enthalpy changes in PU50 nanocomposites decreased with the increasing amount of BZD-Mont, resulting from the presence of layered silicates in polyurethane actually serving as nucleation sites at the beginning of the crystallization of polyurethane, but preventing the growth of the hard-segment domain or becoming a crystallization retardation agent in the later stage of the crystallization process. As for the PU63 nanocomposites, the enthalpy changes due to the long-range-order disruption (ΔH_L) increased from 5.6 J/g in PU63 to 23.4 J/g in 5/95 BZD-Mont/PU63 nanocomposites. This result implies that the dispersed silicate layers constrained the disruption process for hard segments of long-range order in PU63. In the PU63 cases, the enthalpy changes due to melting were reduced from 14.6 J/g for pure PU63 to 1.0 J/g for 5/95 BZD-Mont/PU63, which can be explained by the same hindered crystallization argument used for BZD-Mont/PU50 nanocomposites. The hindrance effect was more pronounced in PU63 nanocomposites than that in PU50 nanocomposites because the density of the hard-segment domains in PU63 was much higher than that in PU50 due to the higher MDI content (molar ratio of MDI = 5/3) in

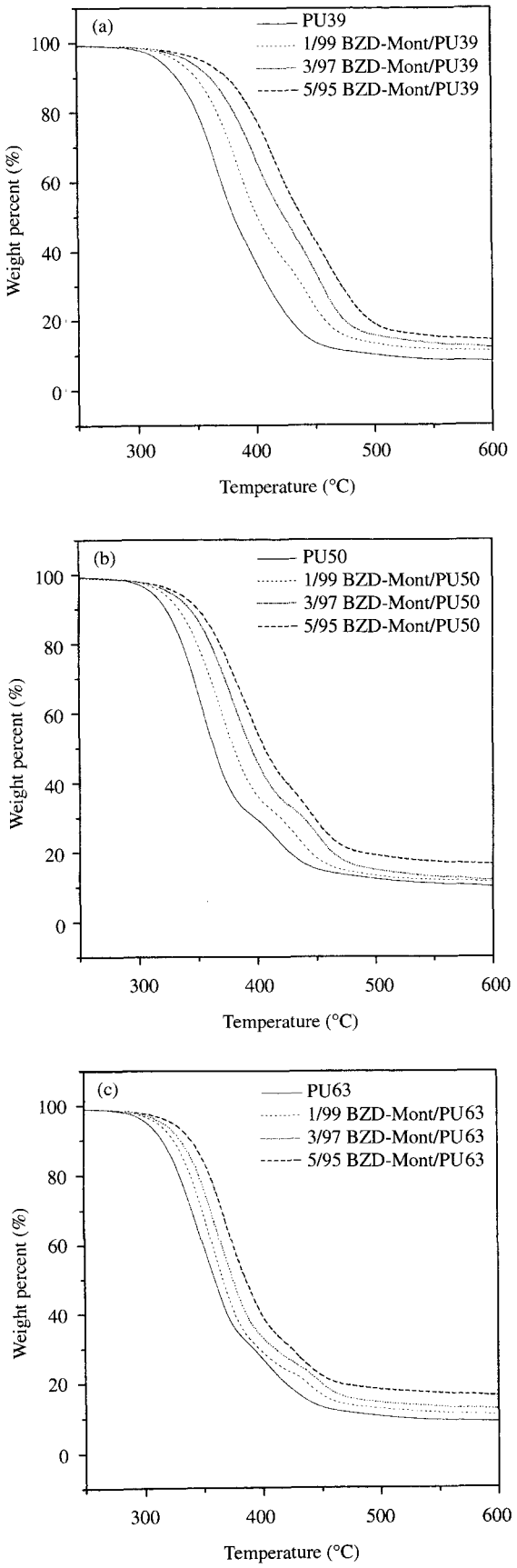

Figure 3. The TGA curves of pristine polyurethane and of BZD-Mont/polyurethane for (a) PU39, (b) PU50, and (c) PU63 cases.

PU63 as indicated in Table I. The silicates were quite large (100 nm in diameter), and they could have covered more hard-segment domains in the case of the higher density of hard segments. Therefore, the disruption effect of silicates on the crystallinity or on the enthalpy change in melting was much greater in PU63 nanocomposites than that in PU50 nanocomposites.

The thermogravimetric analysis curves of BZD-Mont/polyurethane nanocomposites of different hard segment contents are shown in Figures 3(a), 3(b) and 3(c), respectively. The degradation temperatures at 5% weight loss are given in Table II. The degradation temperature of PU39 was 320 °C and decreased to 311 and 302 °C for PU50 and for PU63, respectively. The increases in the degradation temperatures of 5/95 BZD-Mont/PU39, 5/95 BZD-Mont/PU50 and 5/95 BZD-Mont/PU63 nanocomposites were 34, 19 and 15 °C, respectively, as compared to those of PU39, PU50 and PU63. The amount of increase in the degradation temperature (heat-resistant effect) of polyurethane nanocomposites by silicates decreased with increasing the amount of hard segment in polyurethane. This is primarily due to a poor dispersion of silicates in polyurethane as the hard segment content of polyurethane increased.

Conclusions

The presence of layered silicates from benzidine-modified montmorillonite in polyurethane of different hard segment contents can result in hard segments having a more thermally stable long-range order and a higher melting temperature, but showing a loss in crystallinity of the hard segment in polyurethane. The degradation temperature of BZD-Mont/polyurethane nanocomposite was slightly higher than that of pure polyurethane.

Acknowledgement

The financial support for this study was provided by the National Science Council of Taiwan through project NSC89-2216-E-009-008.

References

1. J. A. Miller, S. B. Lin, K. S. Hwang, K. S. Wu, P. E. Gibson and S. L. Cooper, *Macromolecules*, **18**, 32 (1985).
2. T. Kajiyama and W. J. Macknight, *Macromolecules*, **3**, 254 (1969).
3. S. Abouzahr, G. L. Wilkes and Z. Ophir, *Polymer*, **23**, 1077 (1982).

4. J. T. Koberstein, A. F. Galambos and L. M. Leung, *Macromolecules*, **25**, 6195 (1992).
5. L. M. Leung and J. T. Koberstein, *Macromolecules*, **19**, 706 (1986).
6. J. T. Koberstein and T. P. Russell, *Macromolecules*, **19**, 714 (1986).
7. W. Hu and J. T. Koberstein, *J. Polym. Sci., Polym. Phys.*, **32**, 437 (1994).
8. Z. S. Petrovic, Z. Zavargo, J. H. Flynn and W. J. Macknight, *J. Appl. Polym. Sci.*, **51**, 1087 (1994).
9. Y. T. Shieh, H. T. Chen, K. H. Liu and Y. K. Twu, *J. Polym. Sci., Polym. Chem.*, **37**, 4126 (1999).
10. A. Usuki et al., U.S. Pat. 4,889,885 (1989).
11. A. Usuki, M. Kawasumi, Y. Kojima, A. Okada and T. Kurauchi and O. Kamigaito, *J. Mater. Res.*, **8**, 1174 (1993).
12. A. Usuki, M. Kawasumi, Y. Kojima, A. Okada, Y. Fukushima, T. Kurauchi and O. Kamigaito, *J. Mater. Res.*, **8**, 1179 (1993).
13. Y. Kojima, A. Usuki, M. Kawasumi, A. Okada, T. Kurauchi and O. Kamigaito, *J. Polym. Sci., Polym. Chem.*, **31**, 983 (1993).
14. K. Yano, A. Usuki, A. Okada, T. Kurauchi and O. Kamigaito, *J. Polym. Sci., Polym. Chem.*, **31**, 2493 (1993).
15. T. Lan, P. D. Kaviratna and T. J. Pinnavaia, *Chem. Mater.*, **6**, 573 (1994).
16. H. L. Tyan, Y. C. Liu and K. H. Wei, *Polymer*, **6**, 573 (1999).
17. H. L. Tyan, Y. C. Liu and K. H. Wei, *Chem. Mater.*, **11**, 1942 (1999).
18. P. B. Messersmith and E. P. Giannelis, *Chem. Mater.*, **5**, 1064 (1993).
19. P. B. Messersmith and E. P. Giannelis, *J. Polym. Sci., Polym. Chem.*, **33**, 1047 (1995).
20. K. E. Yangchuan, L. Chenfen and Q. I. Zongneng, *J. Appl. Polym. Sci.*, **71**, 1139 (1999).
21. Z. Wang and T. J. Pinnavaia, *Chem. Mater.*, **10**, 3769 (1998).
22. C. Zilg, R. Thomann, R. Mulhaupt and J. Finter, *Adv. Mater.*, **11**, 49 (1999).
23. T. K. Chen, Y. I. Tien and K. H. Wei, *J. Polym. Sci., Polym. Chem.*, **37**, 2225 (1999).
24. T. K. Chen, Y. I. Tien and K. H. Wei, *Polymer*, **41**, 1345 (2000).
25. Y. I. Tien and K. H. Wei, *Polymer*, accepted.